JOURNAL OF CATALYSIS **160,** 19–26 (1996)
ARTICLE NO. 0119

Ethylene Oxidation over Platinum: *In Situ* Electrochemically Controlled Promotion Using Na–β'' Alumina and Studies with a Pt(111)/Na Model Catalyst

Ian R. Harkness,*[,1] Christopher Hardacre,*[,2] Richard M. Lambert,*[,3] Ioannis V. Yentekakis,† and Constantinos G. Vayenas†

*Chemistry Department, Cambridge University, Cambridge CB2 1EW, England; and †Department of Chemical Engineering, University of Patras, Patras 26500, Greece

Received July 31, 1995; revised December 29, 1995; accepted January 4, 1996

Electrochemically modified ethylene oxidation over a Pt film supported on the Na^+ ion conductor β'' alumina has been studied over a range of conditions encompassing both promotion and poisoning. The system exhibits reversible behavior, and the data are interpreted in terms of (i) Na-enhanced oxygen chemisorption and (ii) poisoning of the surface by accumulation of Na compounds. At low Na coverages the first effect results in increased competitive adsorption of oxygen at the expense of ethylene, resulting in an increased rate. At very negative catalyst potentials (high Na coverage) both effects operate to poison the system: the increased strength of the Pt–O bond and coverage of the catalytic surface by compounds of Na strongly suppress the rate. Kinetic and spectroscopic results for ethylene oxidation over a Pt(111)-Na model catalyst shed light on important aspects of the electrochemically controlled system. Low levels of Na promote the reaction and high levels poison it, mirroring the behavior observed under electrochemical control and strongly suggesting that sodium pumped from the solid electrolyte is the key species. XP and Auger spectra show that under reaction conditions, the sodium exists as a surface carbonate. Post-reaction TPD spectra and the use of ^{13}CO demonstrate that CO is formed as a stable reaction intermediate. The observed activation energy (56 ± 3 kJ/mol) is similar to that measured for CO oxidation under comparable conditions, suggesting that the rate limiting step is CO oxidation.

INTRODUCTION

Electrochemical promotion (EP)provides a novel and highly controllable means of altering the performance of heterogeneous catalysts. The applicability of this phenomenon to a range of metal-catalyzed reactions has been demonstrated by Vayenas *et al.*, both for gas/solid systems (1 and references therein), and for reactions taking place in solution (2). The behavior of these systems may be quantitatively rationalized in terms of changes in adsorption energies (and therefore reaction activation energies) caused by changes in catalyst work function which result from backspillover of electrochemically pumped ions from a solid electrolyte to the active metal component. The electrochemically induced rate changes are strongly non-Faradaic in that they are up to five orders of magnitude greater than the rate of ion transport through the solid electrolyte. Independent laboratories have also reported the EP phenomenon for benzene hydrogenation (3), methane oxidation (4), and reduction of NO by ethylene (5).

Bebelis and Vayenas (6) have carried out a detailed study of the EP behavior of ethylene oxidation over polycrystalline Pt films supported in yttria-stabilized zirconia (an oxygen ion conductor) using a fuel cell type tube reactor. More recently (7), Yentekakis and Bebelis showed that this catalytic system could also be studied successfully with a single pellet geometry, which is more readily applied in conventional flow reactors. In both cases it was found that pumping oxygen ions *to* the Pt surface led to large *increases* in the rate of ethylene combustion. Vayenas *et al.* have also studied the reaction in a tube reactor (8) using Pt films deposited on a different solid electrolyte, β'' alumina, which is a sodium ion conductor. This was the first report of electrochemical promotion with a Na^+ conductor. Under their conditions, *supplying* Na to the catalyst led to strong *attenuation* of the reaction rate, which over a certain regime decreased exponentially with catalyst work function: this is consistent with the opposite behavior exhibited under oxygen pumping and in line with the explanation offered for EP in terms of the effect on catalyst work function. The Pt/β'' alumina system is potentially more complex than the corresponding Pt/zirconia system because of the possibility of stable surface compound formation between the electrochemically pumped species (Na) and the reactant gases. The importance of such effects has already been shown in the case of EP CO oxidation over Pt/β'' alumina (9).

[1] Present address: Department of Chemistry, University of Edinburgh, Kings Buildings, West Mains Road, Edinburgh EH9 3JJ.
[2] Present address: Department of Chemistry, Queen's University of Belfast, Belfast, BT9 5AG.
[3] To whom correspondence should be addressed.

0021-9517/96 $18.00

Here we report a further study of ethylene combustion over Pt/β'' alumina. The data presented here confirm the main features observed in the earlier work in which a different type of reactor was used. New aspects of the present work are (i) application of a pellet geometry flow reactor, (ii) observation of electrochemical *promotion* of ethylene combustion when Na is supplied to the catalyst, and (iii) kinetic and spectroscopic experiments with Pt(111)/Na model catalysts which shed light on certain aspects of the EP system. In particular, the single crystal results provide strong support for the central hypothesis of the Vayenas model, namely that changes in catalyst behavior are due to backspillover of electrochemically pumped species—in this case Na.

METHODS

Electrochemical studies at atmospheric pressure were performed in a CST reactor (volume 60 cm^3), product analysis being carried out by means of Balzers QMG 064 quadrupole mass spectrometer. A schematic of the reactor cell is shown in Fig. 1. A porous but continuous thin film Pt working electrode (the catalyst) and Au reference and counterelectrodes were deposited on a disk of β'' alumina (2.8 mm thick $\times$ 16 mm diameter) following the method described previously (9). The thickness of the 12 mm diameter catalyst film was ≈ 5 μm and the total Pt loading on the β'' alumina wafer was $\sim$1 mg. Catalytic rate measurements under potentiostatic and galvanostatic conditions were carried out using an Amel type 553 galvanostat–potentiostat. Most observations were carried out in potentiostatic mode by following the effect of the potential difference between the catalyst and the reference electrode (V_{wr}) on the reaction rate. O_2 (20%) in He, He (Distillers MG), and ethylene (B.O.C.) were fed to the reactor without further purification.

Complementary experiments were carried out using a Pt(111) single crystal model catalyst which could be translated between a UHV chamber (XPS, TPD, Na dosing, Ar^+ etching) and pressure cell (30 cm^3) which could be operated as a differential batch reactor. Reactant and product concentrations were monitored mass spectrometrically (VG Q7) and the elapsed time between pumping out the reactor and transferring the sample to a UHV environment was typically 10 min. TPD spectra were recorded in multiplexed mode with a heating rate of 20 K/s. XP spectra were acquired with a VSW HA-100 instrument using Mg $K\alpha$ radiation and electron binding energies were referenced to the Pt $4f_{7/2}$ peak at 71.1 eV. Sodium was dosed from a collimated evaporation source (SAES Getters). The sodium source was calibrated using uptake data determined by TPD. The deposition time corresponding to a monolayer was identified by the appearance of the distinctive sharp low temperature multilayer peak in the sodium TPD. Corresponding Na 1*s* and Pt 4*f* XP spectra were measured, and the Na 1*s*/Pt 4*f* intensity ratio was taken as a fingerprint of sodium coverage. This procedure eliminated the need for recalibration of the source as it became exhausted during the course of the work. It should be noted that 1 monolayer of sodium on Pt(111) is equivalent to a coverage of Na/Pt of 0.59 (10). Note that in any given experiment an equal amount of Na was deposited on *both* surfaces of the Pt(111) wafer.

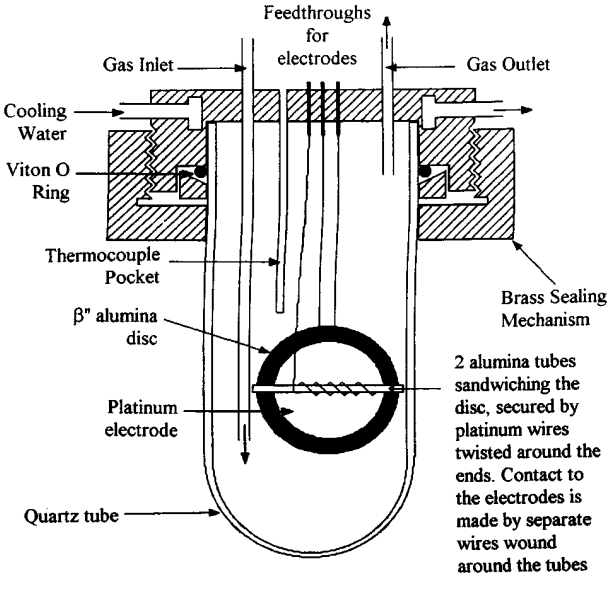

FIG. 1. Schematic of EP reactor.

RESULTS

CST Reactor

The surface area of the catalyst was estimated by two independent methods. The first involved carrying out a CO oxidation control experiment under conditions for which the turnover frequency had been accurately determined previously (9) ($T = 350°C$, $P_{O_2} = 6$ kPa, $P_{CO} = 2$ kPa). This gave a value for the active surface area of 1.1×10^{-6} mol of platinum ($\sim$430 cm^2). In the second method the sample was initially held at a high positive bias in a pure He atmosphere and a constant negative current was passed through the sample while monitoring the catalyst potential. The surface area of the catalyst film may be conveniently estimated from the initial rate of change of the voltage between the catalyst and the reference electrode (V_{wr}) which is equal to the rate of change of catalyst work function with Na coverage (8, 9) caused by backspillover of sodium ions from the electrolyte to the platinum surface. The initial change in V_{wr} is given by

$$\frac{ed(V_{wr})}{dt} = eP_0\frac{dC_{Na}}{dt} = \frac{eP_0 I}{\varepsilon_O e A_c} = \frac{P_O I}{\varepsilon_0 A_c}, \qquad [1]$$

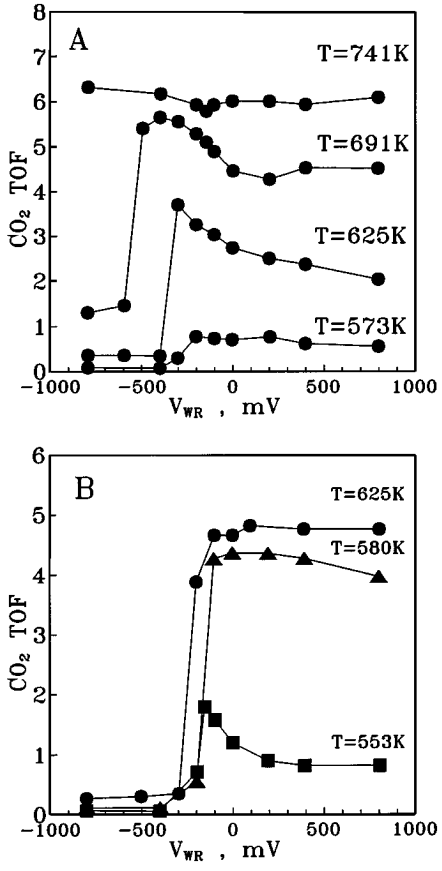

FIG. 2. CO_2 TOF as a function of V_{wr} for (A) 8.0 kPa O_2, 4.2 kPa ethylene and (B) 16.9 kPa O_2, 4.2 kPa ethylene mixtures in the temperature range 553–740 K.

where I is the current, C_{Na} is the atoms of sodium/m^2, P_0 is the initial dipole moment of sodium on platinum ($=2.75 \times 10^{-29}$ cm), A_c is the surface area of the catalyst in m^2 (8, 1), and e and ε_0 take their usual values.

This procedure yields a value of 1.8×10^{-6} mol of platinum ($\sim$710 cm^2) and the two methods therefore yield reasonably consistent results.

Figure 2A shows the reaction rate at four different temperatures in the interval 553–740 K as a function of V_{wr} for an O_2 : ethylene stoichiometry of 2 : 1, and Fig. 2B shows similar data obtained in a more fuel lean system (O_2 : ethylene stoichiometry of 4 : 1). The rate data presented in this figure and in the succeeding figures are given as turnover frequencies (TOF) quoted as molecules of CO_2 production per Pt atom per second.

Using a mean value of 1.5×10^{-6} mol for the active Pt surface area, the CO_2 TOF ranges from 0.13 to 6.8 molecules/Pt site · s, with a zero potential value of ≈ 0.9 at 573 K. These results compare well with those obtained under similar conditions by Vayenas *et al.* using a different reactor configuration (tube geometry (8)). The general S-shape of the TOF vs potential curves reproduces the earlier work, with the upper limb showing a sixfold rate enhancement (8). However, some interesting new features are also observed, in particular the Na-promoted rate enhancement that occurs at moderate sodium coverages and precedes the precipitous fall at more negative biases (i.e., at the highest sodium coverages).

As discussed below, spectroscopic and TPD data obtained with the Pt(111)/Na model catalyst clearly indicate that for all Na precoverages, exposure to reaction conditions results in extensive oxidation of the Na overlayer to yield surface compounds whose nature is discussed below. As does Na itself, these surface compounds induce decreases in the workfunction of the system (11). In order to make contact between the model catalyst and EP-CSTR rate data, we estimate the Na coverages that are present under reaction conditions, coulometrically, from the behavior under a galvanostatic transient obtained *under reaction conditions*. For the sake of brevity we refer to sodium coverage, although it should be understood that this implies coverage of some surface compound of sodium. The Na coverages so computed are subject to an uncertainty factor of $\sim$2 due to the uncertainty in the initial dipole moment to be associated with the Na compound. In earlier work in this laboratory on the CO + NO reaction where similar sodium compounds are believed to form, the initial rate of change of V_{wr} under reaction conditions was approximately half that under helium (12, 13).

The transient behavior of V_{wr} shown in Fig. 3 very closely follows that reported earlier using a fuel cell type tube reactor (8) and we analyze it as described previously by Vayenas *et al.* First, the surface was electrochemically cleaned of Na by application of a positive potential (V_{wr}) on the order of 300 mV until the current ($i > 0$) between the catalyst and counter electrode vanished. Then, the galvanostat was used to impose a constant current $I = -100\ \mu A$ at $t = 0$; this pumped Na to the catalyst surface at a rate $I/F = 1.04 \times 10^{-9}$

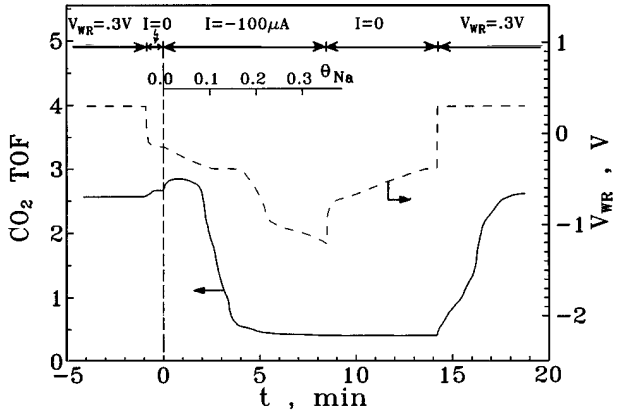

FIG. 3. CO_2 TOF and V_{wr} under a galvanostatic transient. Na coverage abscissa is based on Eq. [1] (see text); Conditions: 8.0 kPa O_2, 4.2 kPa ethylene.

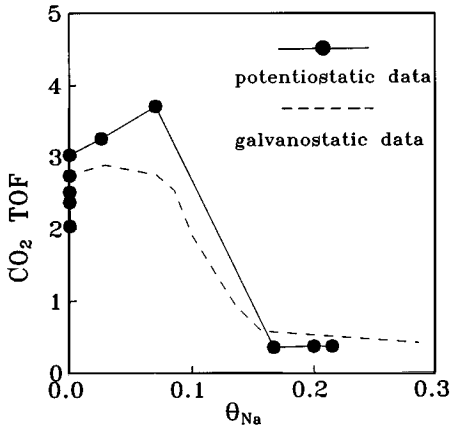

FIG. 4. Rate as a function of Na coverage for both potentiostatic and galvanostatic experiments for a 8.0 kPa O_2 : 4.2 kPa ethylene mixture at 625 K.

mol Na/s. The corresponding Na coverage on the Pt surface (θ_{Na}; Na atoms per Pt surface atom) can be computed from Faraday's law,

$$\frac{d(\theta_{Na})}{dt} = \frac{I}{FN_0}, \qquad [2]$$

where N_0 is the number of available Pt sites (1.5×10^{-6} mol Pt) independently measured as described earlier. This permits construction of the θ_{Na} abscissa used in Figs. 3 and 4.

Thus under transient conditions, increasing θ_{Na} causes a decrease in V_{wr} (and workfunction) and, initially, an *increase* in catalytic rate—in agreement with the steady state behavior shown in Fig. 2A. At $\theta_{Na} \sim 0.07$, continued transport of Na to the surface results in a sharply decreasing rate which eventually falls well below the initial value. Setting $I = 0$ restores V_{wr} to ~ -300 mV while the rate remains unaffected; restoration of the initial rate requires potentiostatic setting of V_{wr} to $+300$ mV (Fig. 3). Note that the transient behavior is fully consistent with the steady state behavior: Na pumping leads to an initial rate increase followed by a sharp decrease. Potentiostatic data and galvanostatic data obtained under the same conditions are compared in Fig. 4.

Pt(111)/Na Model Catalyst

Kinetic experiments were conducted using reactant partial pressures and Na coverages comparable to those used in the CSTR-EP experiments. However, the need to operate the single crystal batch reactor at low conversions (< 5%) restricted the temperature regime to <550 K. The only products found were CO_2 and H_2O. In addition to rate data, we obtained post-reaction XPS, AES, and TPD spectra in order to examine species retained on the Pt surface in the absence and presence of Na. Figure 5 shows post-reaction TPD analysis of the Pt(111) model catalysts after running the reaction over an initially clean surface (3.6 kPa O_2, 1.6 kPa C_2H_4). The sample was cooled to room temperature and the cell pumped out prior to sample transfer and acquisition of the desorption spectra (elapsed time ~10–15 min). The only species detected in desorption after this procedure was carbon monoxide: no desorption of water or of the reactants was found. The α-CO peak (Fig. 5) is due to CO chemisorbed on clean Pt sites (14). The broad feature labeled β is not characteristic of molecular CO desorption from Pt(111). It occurs in a temperature regime associated with the associative desorption of CO resulting from the recombination of C and O adatoms (15) and we assign it accordingly.

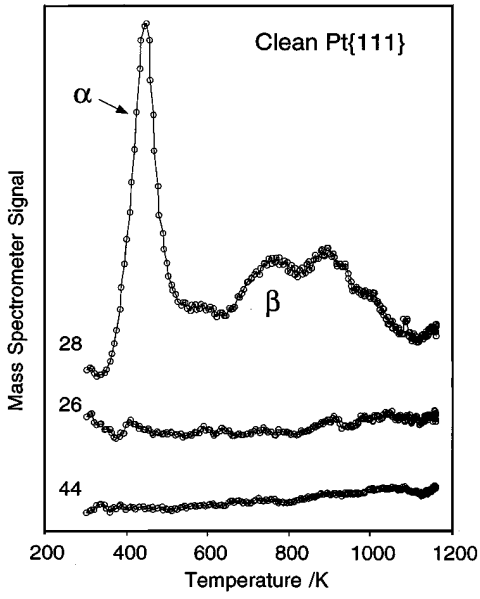

FIG. 5. TPD fingerprint following the reaction of 3.6 kPa O_2 and 1.6 kPa C_2H_4 over clean Pt(111) at 370–420 K.

The question arises as to whether this CO desorption fingerprint is actually diagnostic of the surface condition following reaction, or whether it is merely an artifact resulting from adventitious adsorption of CO present in trace amounts in the residual gas during reactor pump-down and sample transfer to the UHV system. In order to test for this possibility, the following control experiment was carried out. Ethylene oxidation was carried out on the clean Pt(111) surface in the standard fashion, but with the deliberate addition of 0.4 kPa of ^{13}CO to the reactant gas mixture. If the ^{12}CO TPD spectrum in Fig. 5 is merely a sampling artifact, then a similar ^{13}CO spectrum should certainly have been observed after the control experiment. In fact, the ^{12}CO fingerprint was unaltered and there was no detectable ^{13}CO desorption after the control experiment. We therefore conclude that post-reaction TPD analysis does indeed convey relevant information about the surface condition at the end of the reaction and that the ^{12}CO detected in the control experiment was formed by a surface reaction.

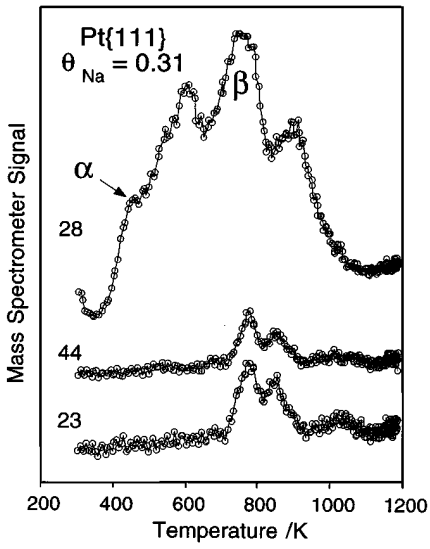

FIG. 6. TPD fingerprint following the reaction of 3.6 kPa O_2 and 1.6 kPa C_2H_4 over Na promoted Pt(111) at 370–420 K ($\theta_{Na} = 0.31$).

Figure 6 shows the post-reaction TPD spectra acquired after ethylene oxidation on the Pt(111) surface after first dosing the latter with 0.5 monolayers (ML) Na. It is apparent that there are major differences compared to the Na-free case. In addition to CO, desorption of Na and CO_2 now occurs and the two peaks in the Na and CO_2 TPD spectra are coincident. The CO fingerprint is much more complex than before: the clean surface α-peak is strongly attenuated and the β features are far more intense than in the Na-free case. Moreover, the high temperature components of the 28 amu β desorption contain a substantial contribution from the CO^+ fragment ion of CO_2. Therefore we assign the coincident peaks in the Na and CO_2 spectra (and the accompanying 28 amu features) to decomposition of surface sodium carbonates (16, 17)

Figure 7 shows the X-ray excited Na KLL Auger electron spectra obtained before and after carrying out the reaction. These clearly point to a change in the chemical nature of the sodium as a result of exposure to the reaction mixture; they also indicate significant loss of sodium within the probe depth of the technique (~4 nm). The position of the peak after reaction is again consistent with the formation of a mixture of sodium carbonate compounds (17). The signal consists of 2 contributions at 990 and 993 eV, due to agglomerated and dispersed material, respectively (17). The degree of loss of sodium superficial area is shown in the first column of Table 1. The coverages were calculated from Na 1*s*/Pt 4*f* intensity ratios as described above. It is clear that agglomeration is significant with the lower coverage overlayer losing 30% of its area and the higher coverage case losing 80%. It should also be noted that the final sodium coverages are similar and less than 1 monolayer in the two cases. The sodium TPD intensity confirmed that the reduction in superficial area cannot be principally attributed to loss of sodium from the surface. However, due to the low signal intensity, minor loss by evaporation cannot be ruled out. Note also that the degree of agglomeration at room temperature may differ from that which prevails at reaction temperature. Figure 8 shows the Na 1*s* XP spectra

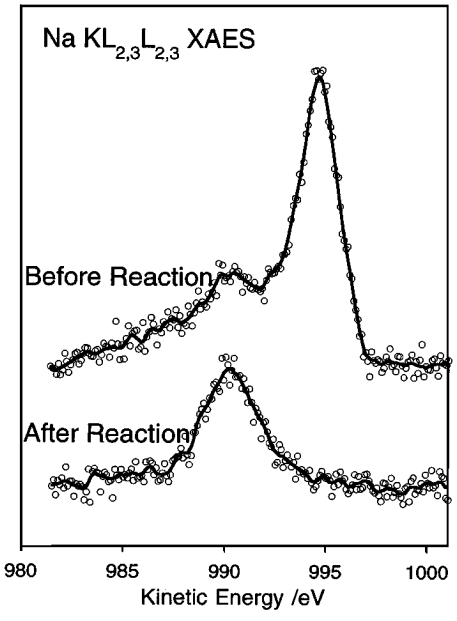

FIG. 7. X-ray excited Na KLL Auger electron spectra obtained (A) before and (B) after ethylene oxidation over Na promoted Pt(111) ($\theta_{Na} = 0.31$).

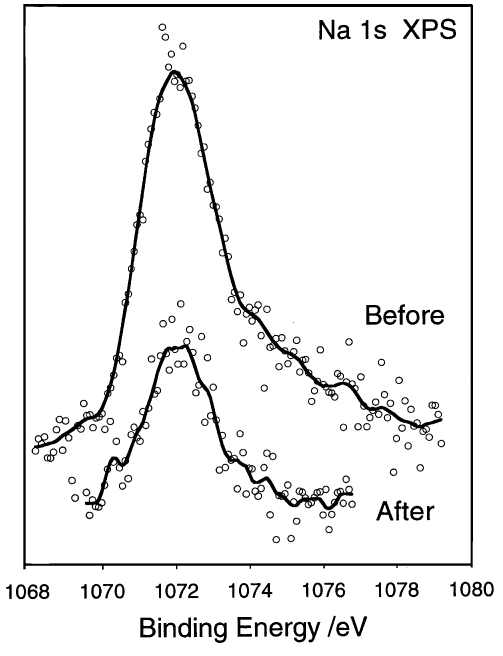

FIG. 8. Na 1*s* XP spectra obtained (A) before and (B) after ethylene oxidation over Na poisoned Pt(111). Initial $\theta_{Na} = 1.8$.

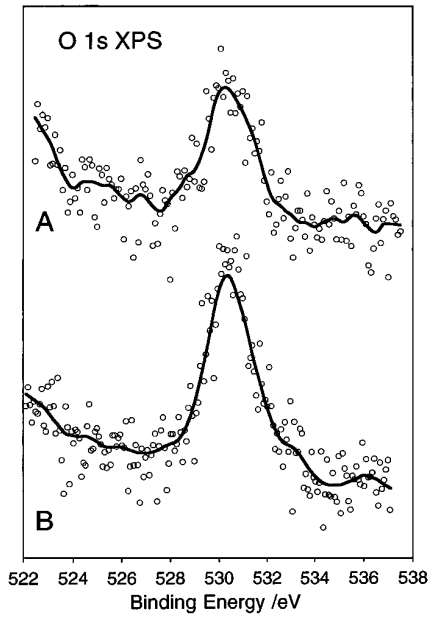

FIG. 9. O 1*s* XP spectra obtained (A) before and (B) after ethylene oxidation over Na Promoted and poisoned Pt(111). Initial $\theta_{Na} = 0.31$.

corresponding to the Auger spectra in Fig. 7: it can be seen that there is little change in the Na 1*s* binding energy before and after reaction. The O 1*s* XP spectrum of the post reaction surface is shown in Fig. 9; it consists of a single peak at 530.5 eV

Kinetic data as a function of Na coverage were obtained with the Pt(111) model catalyst over the temperature regime 370–540 K using the batch reactor. In each case the initial gas composition was 3.6 kPa O_2 and 1.6 kPa C_2H_4. Kinetic parameters extracted from these rate data are shown in Table 1. The submonolayer dose of sodium caused a 25% increase in rate as compared to the sodium-free surface. At higher sodium coverages the rate was depressed to one third that of the sodium-free surface. The apparent activation energies in all three experiments were equal within error, at 56 ± 3 kJ/mol.

TABLE 1

Kinetic Parameters of Ethylene Oxidation over the Pt(111) Model Catalyst

Sodium coverage (Na/Pt)		In (preexponential)	Activation energy (/kJmol^{-1})	Turnover frequency at 413 K ±4%
Initial	Final			
0	0	11.4	59	1.2×10^{-3}
0.31	0.22	10.5	56	1.5×10^{-3}
1.8	0.30	7.2	53	4.0×10^{-4}

DISCUSSION

The steady state EP–CSTR data exhibit the following key features. At relatively low temperatures (550–690 K) and for low levels of Na pumping to the catalyst ($V_{wr} =$ 0–400 mV; $\theta_{Na} = 0$–0.1) the rate exhibits Na-induced promotion. The maximum value of $r/r_0 \sim 2$ occurs at 625 K and $V_{wr} = -300$ mV. For all temperatures in this interval, increased Na pumping eventually leads to a steep decline in rate at $V_{wr} < -400$ mV; we shall refer to this as the poisoned regime. At sufficiently high temperatures, the promoting the poisoning effects are both quenched. The overall response of the system may be understood in terms of the interplay of the following factors: oxygen coverage, Pt–oxygen bond strength, and the effects of Na surface compound formation.

The promotion observed at relatively low temperatures and moderate sodium coverages can be rationalized in terms of the work function dependent adsorption model of Vayenas *et al.* (1). The sodium induced work function decrease results in increased oxygen surface coverage and decreased ethylene coverage as a consequence of increasing and decreasing adsorption energy, respectively. The competitive adsorption of oxygen will thus be enhanced, and, since the reaction has been shown to be first order in oxygen under these conditions (1), an increased rate will result.

At sufficiently large negative values of V_{wr} (sufficiently low work function) the adsorption enthalpy of oxygen increases to the point where increased activation energy for its reaction with ethylene becomes the dominant factor. This leads to an exponential decline in rate, as discussed previously (for example reference 7). Furthermore, as is apparent from Fig. 3, in this regime of V_{wr} the value of θ_{Na} is changing rapidly and nonlinearly with V_{wr} (a consequence of the usual decrease in dipole moment with coverage of polar adsorbed species). That is, the surface becomes extensively blocked with the Na surface compound(s). The net result of these two effects is a very sharp cutoff in rate with decreasing V_{wr}, as observed experimentally. The transient data agree qualitatively with the steady state data in that they show an initial promotion followed by poisoning, as Na is pumped to the catalyst (Fig. 3). The two types of results are in reasonable quantitative accord, as illustrated in Fig. 4, which also demonstrates that on the experimental time scale the system is in a dynamic steady state at all points along the galvanostatic transient.

At sufficiently high temperatures, the Na surface compounds are thermally unstable and cannot be retained on the surface, as can be seen from the desorption temperatures in Fig. 6; the poisoning at $V_{wr} \approx -400$ mV should therefore be quenched as is found in practice (Fig. 2A). In line with this, note that the catalyst potential required for the onset of poisoning becomes more negative with increasing temperature, presumably due to increased

rate of loss of sodium compounds by desorption. Analogous temperature-dependent behavior is exhibited by the $CO + O_2$ reaction under EP over Pt/β'' alumina (9) where it may be rationalized in terms of the formation and destruction of Na–CO surface complexes (18), although recent work in our laboratory suggests that carbonates may also be responsible in this case as well (17).

The results obtained with the Pt(111)/Na model system shed useful light on the catalytic consequences of Na dosing, the identity and thermal stability of the alkali compounds formed under reaction conditions, and the intermediate steps involved in the overall oxidation process. We also obtain insight into the ultimate fate of the electrochemically pumped Na under steady state conditions. Most importantly, the single crystal measurements strongly support the key hypothesis of the Vayenas model, namely that electrochemical promotion is the result of ion backspillover (Na in this case) from the electrolyte to the metal catalyst. Thus we find that when sodium is deposited on Pt(111) from the gas phase, low coverages of Na promote the reaction and high coverages poison it—in accord with the EP results.

The pre- and post-reaction Na KLL Auger spectra clearly indicate that extensive oxidation of the Na overlayer occurs under reaction conditions: this is to be expected. Note that the corresponding Na 1*s* XP spectra do not exhibit an appreciable chemical shift after reaction; this Auger/XPS behavior is fully consistent with literature reports of the spectral changes observed upon oxidation of Na. The post-reaction O 1*s* XP spectra indicate the presence of carbonate. Moreover, the post-reaction TPD results, supported by control experiments with coadsorbed Na, CO_2, and oxygen, indicate that the surface compounds formed under these conditions are actually carbonates (17). The TPD peak temperatures are in the range observed for carbonates formed by dosing a sodium precovered Pt(111) sample with CO_2 and O_2 (17). The exact temperature of desorption was found to depend on the sodium: $CO_2 : O_2$ stoichiometry with the presence of O_2 stabilizing the compound, in accordance with observations on K/Pt(111) (16). The presence of two peaks therefore suggests a degree of surface inhomogeneity, some areas being relatively oxygen rich compared to others.

The CO post-reaction TPD results, especially those obtained when ^{13}CO and ethylene were co-oxidized, strongly suggest that CO is present as a stable absorbed intermediate which is formed during ethylene oxidation. Although there have been UHV TPR studies which show that CO is produced when coadsorbed hydrocarbons and O_2 are allowed to react (19), the present results appear to be the first instance of CO being found as a surface intermediate during hydrocarbon oxidation under practical conditions of true catalytic turnover. In this connection, the kinetic data are of interest. Under our conditions ($CO : O_2 \sim 2.25$) the apparent activation energy for ethylene oxidation is 56 ± 3 kJ/mol which is close to the value of 54.4 kJ/mol reported for CO oxidation over Pt at 450 K (20) under similar conditions. This lends further credence to the view that CO is formed as an adsorbed intermediate during the overall oxidation reaction. The fact that the rate falls at higher sodium coverages suggests that a site blocking mechanism contributes to the reduction in activity: This is consistent with the decrease in free Pt area (from CO TPD). The most likely species responsible for blocking the active sites is sodium carbonate. The post-reaction *apparent* coverage of sodium in the poisoned regime is however of the same order as the sodium promoted case which could indicate that sodium is not the primary cause of loss of free Pt area, and that some other material also contributes to site blocking. Recall, however, that the post-reaction coverages measured at room temperature may not faithfully reflect the dispersion of the carbonate at reaction temperature. No tests were carried out to establish whether partial agglomeration/redispersion of Na compounds occurred reversibly as a function of temperature. This could be established unambiguously only by some kind of *in situ* measurement. Similar post-reactor data obtained with Ag/alumina catalysts indicate that the cesium promoter is mobile under reaction conditions, and the authors were led to conclude that promoter agglomeration upon cooling did not occur (21). However, there are no other data available which allow one to assess whether this is a general rule. In addition, it is not clear whether the Ag/alumina results refer to the state of promoter on the metal, the support, or both. Comparable amounts of carbon deposition were observed by Auger spectroscopy after reaction in all our experiments, and it seems probable that carbon deposition also occurred on the EP catalyst under reaction conditions, so the two sets of data should be comparable in this respect also. Recently, this has been confirmed by post-reaction XPS observations on a Pt/β'' alumina catalyst used for EP propene oxidation (22).

CONCLUSIONS

1. Submonolayer amounts of sodium compounds promote the oxidation of ethylene over Pt(111); larger amounts poison the reaction.

2. Ethylene oxidation on a Pt/β'' alumina catalyst is promoted by the electrochemical pumping of moderate amounts of sodium toward the catalyst surface; larger amounts cause the reaction to be poisoned.

3. Over the same regime of sodium coverages the kinetic behavior of the EP catalyst agrees with that of the Pt(111)/Na model catalyst. This constitutes strong evidence that Na is indeed the key promoting species under conditions of electrochemical control.

4. Under C_2H_4-rich conditions, the apparent activation energy for reaction on Pt(111) is $\sim$56 kJ/mol. This value and the formation of CO as a reaction intermediate suggest

that CO oxidation is the rate determining step in ethylene oxidation.

ACKNOWLEDGMENTS

I.R.H. acknowledges the award of SERC Research Studentship 90316638. C.H. holds an EPSRC Research Fellowship and is a Research Fellow of Emmanuel College, Cambridge. We thank the British Council for the award of Joint Research Grant ATH/882/2/FUEL.

REFERENCES

1. Vayenas, C. G., Bebelis, S., Yentekakis, I. V., and Lintz, H.-G., *Catal. Today* **11**, 303 (1992).
2. Neophytides, S. G., Tsiplakides, D., Stoneheart, P., Jaksic, M. M., and Vayenas, C. G., Nature **370**, 45 (1994).
3. Cavalca, C. A., and Haller, G. L., submitted for publication.
4. Marina, O., Sobyanin, V. A., Belyaev, V. D., and Parmov, V. N., *Catal. Today* **13**, 567 (1992).
5. Harkness, I. R., and Lambert, R. M., *J. Catal.* **152**, 211 (1995).
6. Bebelis, S., and Vayenas, C. G., *J. Catal.* **118**, 125 (1989).
7. Yentekakis, I. V., and Bebelis, S., *J. Catal.* **137**, 278 (1992).
8. Vayenas, C. G., Bebelis, S., and Despotopoulou, M., *J. Catal.* **128**, 415 (1991).
9. Yentekakis, I. V., Moggridge, G., Vayenas, C. G., and Lambert, R. M., *J. Catal.* **146**, 292 (1994).
10. Cousty, J., and Riwan, J, *Surf. Sci.* **204**, 45 (1988).
11. Bonzel, H. P., *Surf. Sci. Rep.* **8**, 43 (1987).
12. Harkness, I. R., and Lambert, R. M., in preparation.
13. Palermo, A., Yentekakis, I. V., Vayenas, C. G., and Lambert, R. M., in preparation.
14. Gland, J. L., and Kollin, B. E., *Surf. Sci.* **151**, 260 (1985).
15. Schäffer, L., and Wassmuth, H. W., *Surf. Sci.* **208**, 55 (1989).
16. Liu, Z. M., Zhou, Y., Solymosi, F., and White, J. M., *Surf. Sci.* **245**, 289 (1991).
17. Harkness, I. R., Ph. D. Thesis, University of Cambridge, 1995.
18. Bertolini, J. C., Delichère, P., and Massardier, J., *Surf. Sci.* **160**, 531 (1985).
19. Steninger, H., Ibach, H., and Lehwald, S., *Surf. Sci.* **117**, 685 (1982).
20. Berlowitz, P. J., Peden, C. H. F., and Goodman, D. W., *J. Phys. Chem.* **92**, 5213 (1988).
21. Mross, W. D., *Catal. Rev.* **25**, 591 (1983).
22. Tikhov, M. S., and Lambert, R. M., in preparation.